Solar-Terrestrial Physics, 2016. Vol. 2. Iss. 1, pp. 78–88, DOI: 10.12737/19880. © INFRA-M Academic Publishing House
Original Russian version A.V. Germanenko, Yu.V. Balabin, B.B. Gvozdevsky, L.I. Schur, et al., published in Solnechno-Zemnaya Fizika. 2016, vol. 2, iss. 1, pp. 56–63, DOI: 10.12737/13500

NATURE OF GAMMA RADIATION VARIATIONS DURING ATMOSPHERIC PRECIPITATION

A.V. Germanenko, Yu.V. Balabin, B.B. Gvozdevsky, L.I. Schur

Polar Geophysical Institute KSC RAS, Apatity, Russia
germanenko@pgia.ru

The Polar Geophysical Institute has developed a complex facility for continuously monitoring various components of secondary cosmic rays. Gamma radiation during precipitation events has been found to increase the year round regardless of the season. A series of experiments has revealed that there is no precipitation pollution by any natural or artificial radionuclides. Radiation spectrum does not have any characteristic lines of elements. We propose a mechanism providing a satisfactory description for this phenomenon.

Keywords: *gamma radiation, precipitation, increase.*

INTRODUCTION

The Polar Geophysical Institute's (PGI) cosmic ray (CR) stations in Apatity and Barentsburg have been continuously monitoring various components of secondary CR for several years. The monitoring is implemented using a complex facility consisting of three neutron detectors for different energy ranges, a charged component detector, and a gamma-ray detector. Shortly after the beginning of the monitoring, a new phenomenon was discovered – an increase in the gamma background during precipitation events. The influence of thunderstorm clouds on secondary CR deep in the atmosphere is a well-known fact [Lidvansky, Khayerdinov, 2007; Mendonça et al., 2011]. The primary cause of the occurrence of an excess CR flux during thunderstorms is particles accelerated by strong electric fields inside a thunderstorm cloud. The influence of ordinary (non-thunderstorm) clouds on a gamma-quantum flux has first been discovered by PGI during monitoring of the low-energy X-ray (gamma) background [Germanenko et al., 2010; Germanenko et al., 2011]. Increases were registered which were generally related to atmospheric precipitation. Notice that in the subarctic region (Apatity) thunderstorms are rare, but increases in the gamma background during precipitation events is observed all year round. It has been established that its increases are not caused by any anthropogenic or natural radionuclides – they result from a change in the interaction between cosmic radiation and the atmosphere [Balabin et al., 2014]. Nevertheless, we assume the electric field of non-thunderstorm clouds to cause the precipitation-associated increases. This field, although not so strong as in thunderstorm clouds, further accelerates charged particles that then produce additional slowing-down X-ray (gamma) radiation reaching the ground level.

Since there is no established boundary separating X-rays from gamma rays (according to some sources, it is the electron rest energy of 510 keV; according to others, the energy from several MeV), both the definitions in this paper are synonyms and their choice in a particular place of the paper depends on a sentence; all the more so because the electromagnetic radiation range (from 20 keV to 5 MeV) of interest deliberately encompasses both the definitions.

Hereinafter in our paper, the definitions are equivalent and imply electromagnetic radiation from 20 keV to 5 MeV.

COMPLEX FACILITY FOR MEASURING RADIATION

By now, the facility described in [Balabin et al., 2014] has been supplemented with important components considerably expanding its potential. A new block diagram of the modernized facility at the CR station in Apatity is shown in Figure 1. It includes a standard neutron monitor, scintillation crystal gamma-quantum detectors (SDR), a lead-free section of the neutron monitor, a charged component detector, and a thermal neutron detector.

The standard neutron monitor is sensitive to neutrons with energies of >50 MeV [Dorman, 1975]. The lead-free section detects neutrons with energies of hundreds of keV; the thermal neutron detector measures thermal neutron fluxes. The X-ray detectors feature NaI(Tl) crystals of size 62×20 mm (small, SDR_s) and 150×110 mm (large, SDR_l). SDR_s has integral channels of >20 and >100 keV. A signal from SDR_l arrives at a discriminator forming integral channels of >200, >600, and >1000 keV, as well as at a 4096-channel amplitude analyzer to provide differential gamma spectra in a range 0.2–5 MeV with the 30-min accumulation time for one spectrum. The charged component detector is comprised of gas-discharge counters STS-6. The counters are arranged into two horizontal rows of eight. The total output from the top row and the output from the coincidence circuit of the bottom and top rows are used. The top row registers the total flux of charged and electromagnetic components and,

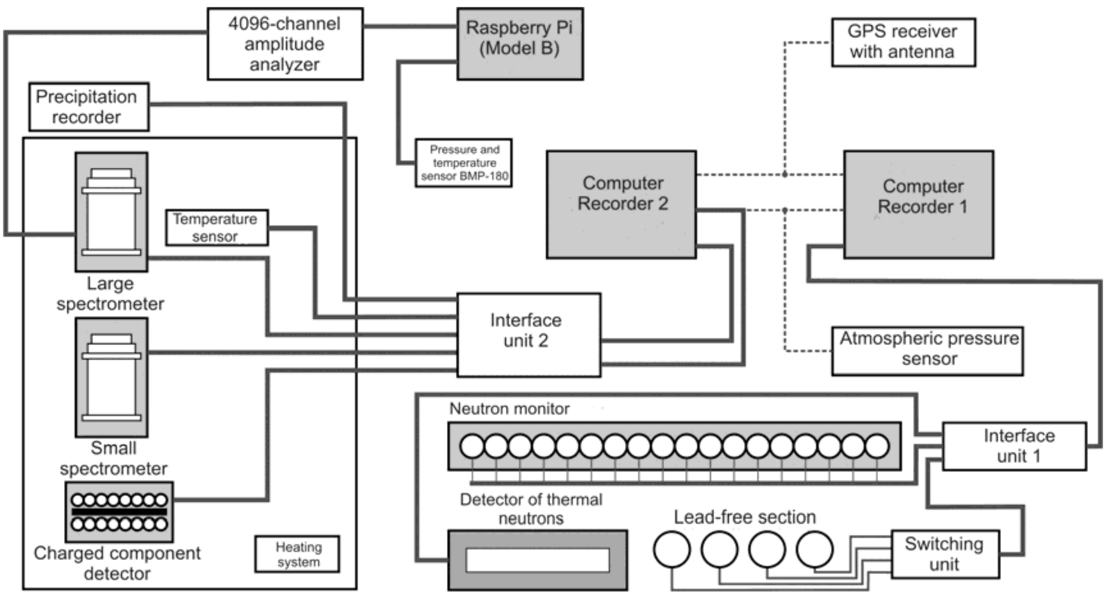

Figure 1. Block diagram of the experimental facility for monitoring secondary CR components in Apatity

because STS-6 have low (around 1 %) efficiency in X-rays [Katsnelson et al., 1985], the coincidence circuit detects only a charged radiation component, i.e. muons and electrons.

Precipitation intensity is measured by a method of infrared backscattering by raindrops or ice crystals. The detector was made at the PGI Laboratory of Arctic Atmosphere [Shishayev, Beloglazov, 2011]. It is not calibrated in absolute units and is exploited only to qualitatively estimate precipitation intensity.

The system also features several temperature and atmospheric pressure sensors. These auxiliary sensors are necessary to apply corrections associated with atmospheric processes to data from detectors.

All the neutron detectors are installed in a one-floor building; the others, in a thermally stabilized box in the attic of this building. SDR_s, SDR_l, and the STS-6 assembly are located in chambers enclosed by lead bricks 50 mm thick. These chambers limit the view of the detectors to an angle of around 140° such that they are screened from background radiation coming from soil and ambient objects.

Continuous observations with the facility have been made at Apatity and Barentsburg (Svalbard) cosmic ray stations since 2010. The complex on Svalbard is still incomplete, but there is SDR_s that shows the same increases in background gamma radiation during precipitation events as in Apatity. The station on Svalbard is important because this archipelago is virtually unpopulated; it has no industry and is situated thousands of kilometers away from populated centers. This is an additional confirmation that the phenomenon we discovered is not caused by radioactive pollution.

GAMMA RADIATION VARIATIONS DURING PRECIPITATION EVENTS

During precipitation events, increases in the gamma background are registered which comprise 50% of background radiation and last several hours. During the observation period (2009–2015), more than 500 such events have been detected altogether. The events occurred both in winter and in summer – regardless of the season. The type of precipitation event (rain or snow) has also little effect on the phenomenon, although winter increases are in general slightly lower than summer ones: in summer there were increases up to 50 %; in winter, 35% at most. The events lasted from 2–3 hours to days and more, depending on duration of a precipitation event. We have revealed a connection between the discovered increase in background gamma radiation and the accompanying weather phenomena. Almost all the increases were followed by heavy precipitation events (rain or snow) and dense, solid clouds with the lower boundary at an altitude of >600 m.

Experiments showed that precipitation was not polluted by any natural or artificial radionuclides [Vashenyuk et al., 2011; Gvozdevsky et al., 2011; Balabin et al., 2014]. Figure 2, *a* (top panel) depicts a typical increase in surface gamma rays according to data from the integral channels. An important peculiarity of the phenomenon is evident: the increase occurs only in the electromagnetic component. The middle panel in Figure 2, *a* illustrates the count rate of the charged component detector (the top row of counters) that remains nearly constant during the event. This is natural because during ordinary rain, clouds have no strong electric fields able to accelerate charged particles. However, as can be seen on the top panel, the gamma-quantum flux increased by 25%.

We employed the method of superposed epochs [Dorman, 1972] to calculate average profiles of the increase in background gamma radiation and precipitation amount. A fixed point was taken to be a precipitation peak, i.e. the profiles were overlaid so that precipitation peaks coincided. For the averaging, we have selected about one hundred events of short duration (no more than 6 hr). Each profile was normalized before being overlaid. As a result, we obtained average profiles of precipitation amount and increase in background gamma radiation (Figure 2, *b*). Precipitation peaked when the radiation flux was most intense, whereas radiation reached a maximum value 30–40 minutes after the precipitation peak. In general, such a relation corresponds to a shock (precipitation) and a response of the inertial system (gamma background) with the mean relaxation time of ~100 min.

Now it is reasonable to address the issue about the nature of the phenomenon, namely the observed effect is not related to any radionuclide pollution of precipitation. This is a definitely established fact. Once, during a heavy rain event with an over 30 % increase, we gathered 5 liters of rainwater (from the roof of the building where the detectors are installed) in a plastic bottle that was immediately (not later than in 10 min) placed over the second SDR_s (Figure 1 does not show this detector for simplicity). This SDR_s is inside a chamber made of lead bricks 5 cm thick, i.e. covered with lead all round, and naturally it does not register any increases. The bottle with water was put over the SDR_s inside the chamber. The detector did not show any changes in the count rate. During another event, we sent 10 liters of rainwater to the KSC RAS Radiological Laboratory to test it for radionuclide pollution. The radionuclide type content and concentration in the water did not differ from background ones for this region. Finally, we outline the following consideration. Turn to Figure 2, *b*.

After cessation of precipitation (including snow that covers the roof directly over the SDR in winter until it falls under its own weight), the X-ray background returns to the normal state for the

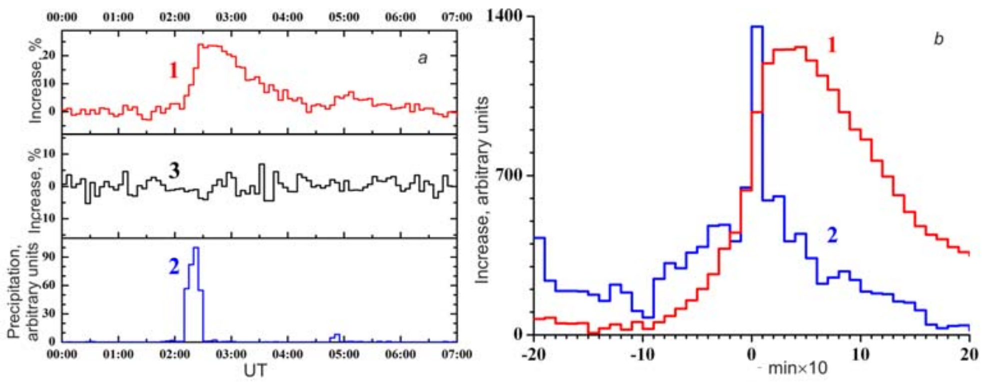

Figure 2. The July 30, 2015 event (*a*): typical profiles of increase in the gamma background, obtained by SDR_s (>100 keV channel (1)) and by the charged component detector (top row of counters (3)), and of precipitation amount (2). Average profiles (*b*) of precipitation amount (2) and increases (1) plotted based on 100 similar events by the method of superposed epochs

characteristic period of ~100 min. If it is granted that the increase was caused by a radionuclide, its half-life would have also been ~100 min. It is difficult to imagine another cause of the radiation intensity decrease with snow on the roof over the detector. Taking the average speed of clouds [Matveev, 1984] into account, we conclude that this radionuclide could enter clouds not farther than at 100 km from the observation point, otherwise it would have decayed by the time the clouds approached the detector. Moreover, the radionuclide should have been continuously produced by the source, or it would have decayed long before the nasty weather. Also notable is that the precipitation related increases are observed in Barentsburg (Svalbard) that has no industry and is situated one thousand kilometers away from the mainland.

ENERGY GAMMA SPECTRA

As previously noted, the monitoring facility has been supplemented with an important component – a large crystal (150×110 mm) detector (SDR_l) – thus enlarging the range of effective monitoring from 400 keV to 5 MeV. SDR_l was calibrated against two sources: ^{137}Cs, the 662 keV line, and ^{60}Co, the 1.17 and 1.34 MeV lines. Besides, the software package GEANT-4 was used to model this detector and calculate the efficiency of registration of gamma-quanta with energies from 100 keV to 5 MeV by the crystal [Maurchev et al., 2015]. These very calculations revealed that this crystal can be employed to register 5 MeV quanta. Reference data [State Standard 20426-82, 1983; Grigoryev, Melikhov, 1991] also showed that radiation in the same energy range can be absorbed by roof coverings (wood and tin). All these were done to correctly transform SDR_l data (count rate) into the initial energy gamma spectrum in the atmosphere.

This crystal is also exploited to continuously measure the differential energy gamma spectrum from 200 keV to 5 MeV. The accumulation time for one spectrum is 30 min. On the one hand, the accumulation time increment improves measuring accuracy, particularly in the high-energy part with low flux intensity; on the other hand, it is desirable to measure a spectrum several times during a short-term event (2–3 hours): at the beginning, maximum, and at the end of the event. The period of 30 min was selected as compromise for these two conditions.

SDR_l measurements of the differential energy spectrum gave an exact answer to the key question concerning the upper energy boundary of the events (increases). Only indirect estimates were possible before [Balabin et al., 2014] because the effective range of SDR_s was narrow and it was clear that the upper energy boundary of the increases was much higher than that of SDR_s (400 keV). SDR_l measurements have revealed that the increase is registered in an energy range of no more than 2–2.5 MeV. The >2.5 MeV quantum flux in precipitation remains unchanged.

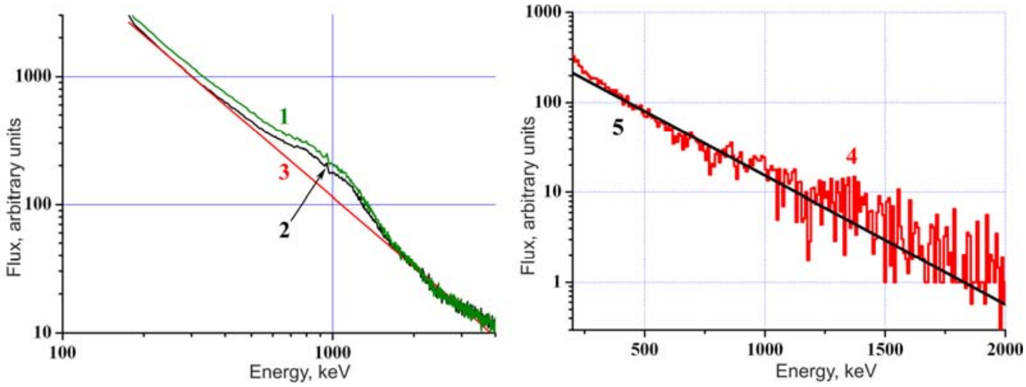

Figure 3. Panel *a* depicts differential energy spectra of background (2) before and during increase (1), as well as approximation (3) of the background spectrum by the power function. Panel *b* is a difference between spectra (1) and (2), which is a spectrum of increase (4), and its exponential function approximation (5)

Direct measurements of the differential spectrum of background gamma radiation coming from the atmosphere from the upper hemisphere have clearly showed that gamma radiation is slowing-down [Gaitler, 1956; Khayakava, 1974]. This is suggested by the power law with γ=1.8. An example of the differential background gamma spectrum is given in Figure 3, *a*. The figure also depicts the spectrum during the event. It is obvious that at energies over 2–2.5 MeV the spectra merge, thus indicating the upper energy boundary of the event. The same value is obtained from exact calculations of the spectrum of increase (Figure 3, *b*). The difference between the differential spectrum measured during the event (curve 1 in Figure 3, *a*) and the spectrum received in clear weather before the increase (curve 2 in Figure 3, *a*) indicates an additional radiation spectrum, i.e. a flux that is superimposed on the background and is registered as an increase.

We have established a vital difference between the background spectrum and the additional radiation spectrum. The latter has an exponential dependence over the 0.2–2 MeV interval. Figure 3, *b* illustrates a typical additional radiation spectrum and its exponential function approximation. Notice that it was the first time the differential spectra of surface gamma background have been estimated and the spectrum of radiation causing the increase in precipitation has been determined.

The finding can be described by the following equations:

$$\begin{cases} I_b(E) = J_0 E^{-\gamma} \text{ — background radiation spectrum,} \\ I_{\text{inc}}(E) = J_1 \exp\left(\dfrac{-E}{E_0}\right) \text{ — additional radiation spectrum,} \end{cases} \qquad (1)$$

where E is the gamma-quantum energy, J_0 is the background flux intensity, γ is the spectral index, J_1 is the intensity of an additional flux emerging during an increase, E_0 is the characteristic energy.

Thus, we can confidently assert that the observed gamma radiation increases accompanied by precipitation events occur in the energy range 0.02–2 MeV (the spectrum in the range 20–400 keV has been previously measured [Balabin et al., 2014]). We have established a vital difference between background radiation always available in Earth's atmosphere and additional radiation emerging in precipitation and adding to background radiation. Background gamma radiation coming from the atmosphere is slowing-down, it has a power law spectrum, emerges in the atmosphere as secondary radiation from CR; its energy is much higher than 5 MeV [Gaitler, 1956; Khayakava, 1974]. This is exactly what is shown by the SDR_l measurements of the background spectrum in the wide range. The energy spectrum of radiation contributing to the increase in precipitation has an exponential shape and the upper boundary 2–2.5 MeV.

The direct measurements of the differential spectrum confirmed our previous conclusion [Balabin et al., 2014] that there are no radionuclides with characteristic lines both in background radiation and in gamma flux increase. All spectra feature a small, extended bulge or bump – a constant excess of quanta with energies of around 1 MeV. However, as indicated by Figure 3, *b*, this bump does not manifest itself at all in additional radiation spectrum (4). This suggests that it is constant for all spectra and is unaffected by gamma radiation increase during precipitation events. The nature of the bump is still unclear.

The differential gamma spectrum has been measured for well over a year, and by now a sufficient number of events have been collected for a comparative study. The observed variations of background radiation related to variations of primary CR flux (especially to Forbush decreases) occur so that the spectral index (γ parameter) remains unchanged. In other words, the slope of the spectral function holds constant, and only flux intensity varies.

For each event, we found a difference between the background spectrum before the event and the spectrum during a maximum increase in gamma flux. The background spectrum was taken not later than 2–3 hr before the beginning of the increase; and, to improve the measurement accuracy, it was averaged over 2–3 hr. This yielded an additional radiation spectrum as in Figure 3, *b*. For this spectrum we determined an approximating exponential function defined by J_1 and E_0. As a result, we obtained an array of these spectral parameters associated with the events. Figure 4 illustrates the distribution of spectral function parameters depending on the increase. Although E_0 exhibits, in our opinion, no relationship with the increase, given a mean value of around 400 keV, J_1 is linearly related to the increase. E_0 and J_1 show no connection between each other. This can lead to the conclusion that precipitation only triggers (or intensifies) a process generating the said radiation, but is not responsible for the process itself.

ENERGY BALANCE AND FURTHER ACCELERATION HYPOTHESIS

Despite increases in gamma intensity have been studied for many years, the mechanism for their generation is still not fully understood. The fundamental hypothesis is the generation of additional slowing-down radiation by light charged particles in the electric field of clouds. Obvious drawbacks of the hypothesis are first that in polar regions thunderstorm activity is low (however, when speaking about acceleration in the electric field of a cloud, we imply the acceleration in a thunderstorm cloud with electric field strength of hundreds of kV/m) and is very rare; in winter there is no such activity at all.

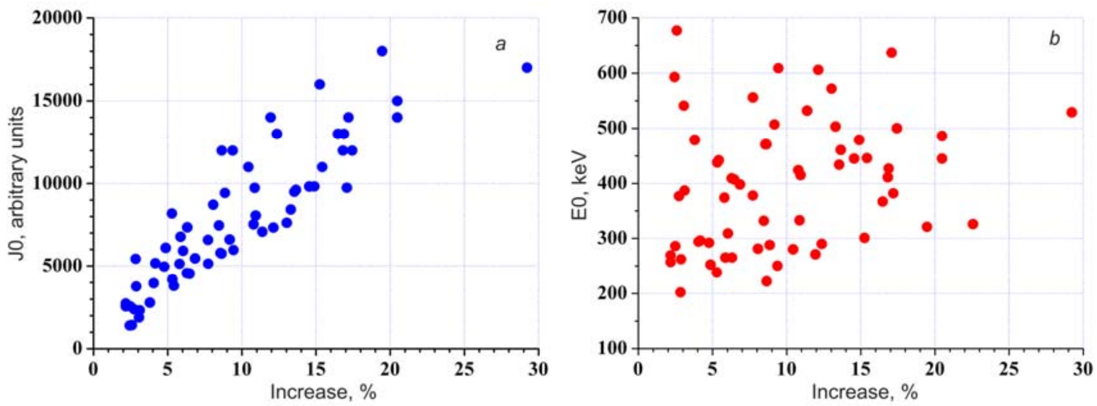

Figure 4. Parameters of the additional radiation spectrum as a function of increase: *a* is a J_1 parameter (flux intensity), *b* is an E_0 parameter (characteristic energy)

Second, the free path of gamma-quanta with energies of hundreds of keV does not exceed 100–300 m [State Standard 20426-82, 1983]; therefore, they can be generated at an altitude of no more than 1 km. However, let us discuss the issue without giving any details so far.

In the atmosphere at any altitude there are light energetic particles (electrons and positrons) [Gaitler, 1956; Khayakava, 1974]. They emerge when secondary cosmic ray components (muons, pions, and gamma quanta) propagate and decay in the atmosphere. When moving in the atmosphere, these light charged particles loss energy in two ways:

$$\begin{cases} dE_{\mathrm{i}} = \sigma_{\mathrm{i}} dx \text{ — ionization losses,} \\ dE_{\mathrm{r}} = \delta E dx \text{ — radiation losses,} \end{cases} \tag{2}$$

where σ_{i} is the specific ionization loss of energy per unit length, δE is the specific radiation loss of energy per unit length, dx is a traveled short distance. Specific ionization losses at energies over 2 MeV very weakly depend on the energy of a particle itself [Gaitler, 1956; Khayakava, 1974], hence σ_{i} can be considered constant. Ionization losses are therefore linear: a double-energy particle travels in a substance twice as long (provided that there are no losses of other types). Specific radiation losses are proportional to particle energy [Gaitler, 1956]. For convenience of description we assume that particle energy decreases according to Equation (2) not over the entire distance dx, but only at its right end (when the distance dx is covered); and the particle goes the distance dx without any changes in its energy. The distance dx being infinitely short, such an assumption changes neither Equation (2) nor the differential description of the process. Now suppose that the particle propagates through an electric field with strength ε. Then (2) becomes

$$\begin{cases} dE_{\mathrm{i}} = \sigma_{\mathrm{i}} dx \text{ — ionization losses,} \\ dE_{\mathrm{r}} = \delta (E + \varepsilon dx) dx \text{ — radiation losses.} \end{cases} \tag{3}$$

The second term in brackets in the second equation in (3) has the second infinitesimal order relative to dx, and its effect must be negligible. But, as stated in [Gaitler, 1956], the feature of radiation losses is that the particle can lose the dE_{r} energy on its way dx with equal probability as a multitude (say, n) of quanta with average energy dE_{r}/n or as one quantum with dE_{r}. The latter means that there exist particles that emit nothing on their way to a point $x_0=mdx$; then they undergo a central collision and eject a quantum with energy of about mdE_r [Gaitler, 1956]. For such particles, εdx in (3) should not be ignored because for them it takes the form εx_0 and has a much larger value. The number of such particles exponentially decreases with increasing distance x_0 traveled. This, by the way, provides the exponential shape for the additional radiation spectrum.

The mechanism for accumulation of additional energy by an energetic particle as it moves in a substance in an electric field and further energy release in course of slowing-down radiation has been termed by us further acceleration. Its peculiarity is that it involves high-energy particles emerging from some other, nonacceleration processes. Low-energy particles cannot gain energy in the electric field in such a dense substance as the lower atmosphere – it is absolutely clear.

Measurements of the differential gamma spectrum carried out at our facility can easily be converted from the relative units "number of pulses per bin" into an absolute energy flux because SDR_l is calibrated and the additional radiation spectrum is bounded. It is necessary only to correctly compare all respective coefficients: crystal size, accumulation time for one spectrum, bin size. As a result we found out, for example, that during a 25 % increase the additional radiation flux Σ_r was ~90 keV $(cm^2 \cdot s)^{-1}$. Here we imply the energy flux from the entire upper hemisphere. In the same way, we can calculate a charged particle flux in this region at this altitude, using measurements made by the charged component detector. The flux Σ_p was ~0.06 of a particle $(cm^2 \cdot s)^{-1}$. Assume that all these are particles involved in further acceleration. In this case, each particle should gain additional energy in the cloud layer

$$\delta E = \frac{\Sigma_r}{\Sigma_p}. \tag{4}$$

Hence δE is the additional energy an energetic particle should obtain in the electric field of a cloud and then emit it as slowing-down radiation to produce at the level of the detector an additional energy flux (in the form of gamma-quanta) equal to Σ_r. In our case, $\delta E \approx 1500$ keV. By accepting that the particle gains this energy when moving in the electric field of clouds and by taking from [Matveyev, 1984] a mean thickness of nimbi h= 500 m, we can estimate the required strength:

$$\varepsilon = \frac{\delta E}{h}. \tag{5}$$

In our case, ε=3 kV/m. Under real conditions, this value can slightly increase. When calculating the spectrum and the energy flux, we took into account coefficients of attenuation of radiation by roof coverings; therefore, the obtained values refer to the energy flux coming from the atmosphere. On the one hand, the measured charged particle flux comprises muons and electrons, rather than only electrons, while slowing-down quanta are ejected only by electrons and positrons. It is known [Gaitler, 1956] that electrons constitute one-third of all charged particles near Earth's surface at sea level, whereas positrons are much less abundant than electrons. Accordingly, ε should be at least three times larger. On the other hand, it is necessary to consider the barometric effect: all components of secondary CR when propagating deep into the atmosphere undergo absorption. Since light charged particles in the atmosphere are produced in several ways (muon decay, pair creation, Compton effect), as an estimate we take the barometric coefficient for muons – the hardest, least absorbed component. At altitudes of around 1 km (the altitude of the lower boundary of clouds 400–600 m plus the cloud thickness of 500 m), the muon flux is 1.5 times higher than that at sea level, and the electron flux increases in approximately the same way. We can concede that the required electric field strength in a cloud, we found from very general assumptions about generation mechanism and energy balance, slightly differs from the real one.

Our estimated electric field strength in nimbi fits into the range obtained from direct measurements: the typical value is 5–10 kV/m; and in some cases, 16 kV/m [Rust, Trapp, 2002]. The experiments were conducted just in nimbostratus clouds representing the basic type of clouds inducing “quiet” (without thunderstorms) precipitation events [Matveev, 1984]. The measurements were made at middle latitudes in different seasons.

Thus, the proposed mechanism for generating additional gamma radiation that involves further acceleration of light energetic particles in electric fields of clouds can work fairly well and is consistent with direct measurements.

CONCLUSION

The PGI Laboratory of Cosmic Rays monitors the surface gamma background in an energy range 0.02–5 MeV. A new phenomenon has been discovered – an increase in the surface gamma background during precipitation events. These increases are observable all year round and during any types of precipitation events. Currently, integral and differential energy gamma spectra are being measured. We have first measured the spectrum of radiation inducing an increase in the gamma background during precipitation events. We revealed that the increases are caused by additional radiation with exponential spectrum, whereas background radiation has a power law spectrum. Besides, we determined the upper boundary of the exponential spectrum that is 2.5–3 MeV. Unlike background radiation with the spectrum ranging to tens of MeV, additional radiation is sufficiently soft.

Using energy balance in the gamma background increases as the base, we have estimated the electric field strength in a cloud required to cause the increases. This estimate does not exceed those from numerous measurements of electric fields in nimbi. We analyzed the results of the experiments and put forward a model consistently describing the mechanism for accumulation and transfer of energy, gained by light charged particles in the electric field of clouds, to the ground level.

REFERENCES

Balabin Y.V., Germanenko A.V., Gvozdevsky B.B., Vashenyuk E.V. Variations in the natural X-ray background in the polar atmosphere // Geomagnetism and Aeronomy. 2014. V. 54, no. 3. pp. 347–356. DOI: 10.1134/S0016793214020029.

Dorman L.I. *Eksperimental’nye i teoreticheskie osnovy astrofiziki kosmicheskikh luchei* [Experimental and

Theoretical Foundations of Cosmic Ray Astrophysics]. Moscow, Nauka Publ., 1975. 463 p. (in Russian).

Dorman L.I. *Meteorologicheskie effekty kosmicheskikh luchei* [Meteorological Effects of Cosmic Rays]. Moscow, Nauka Publ., 1972, 211 p. (in Russian).

Germanenko A.V., Balabin Yu.V., Vashenyuk E.V., et al. Natural gamma background variations during precipitation. *Vestnik Kol'skogo Nauchnogo Tsentra RAN* [Bulletin of Kola Science Centre of RAS]. 2010, iss. 3, pp. 104–109 (in Russian).

Germanenko A.V., Balabin Yu.V., Gvozdevsky B.B., et al. High-energy photons connected to atmospheric precipitations // Astrophys. Space Sci. Trans. 2011, vol. 7. pp. 471–475. DOI: 10.5194/astra-7-471-2011.

GOST 20426-82. Kontrol' nerazrushayushchii. Metody detektoskopii radiatsionnye. Oblast' primeneniya. [State Standard. 20426-82. Non-destructive testing. Methods of defectoscopy radiation. Field of application]. Moscow, Standartinform Publ., 1983, 23 p. (in Russian).

Grigoriev I.S., Melihov E.Z. *Fizicheskie velichiny: spravochnik* [Physical Values: Handbook]. Moscow, Energoatomizdat Publ., 1991, 1231 p.

Gvozdevsky B.B., Balabin Yu.V., Germanenko A.V., Vashenyuk E.V. On the origin of X-ray increases during precipitations // Proceedings of ICRC-2011. 2011, vol. 11, id 0863, pp. 397–400.

Hayakawa S. Cosmic Ray Physics. Nuclear and Astrophysical aspects. New York, Wiley-Interscience, 1969, 774 p. (Russian edition: Hayakava S. *Fizika kosmicheskikh luchei* [Physics of Cosmic Rays]. Moscow, Nauka Publ., 1974, 1042 p.).

Heitler W. The Quantum Theory of Radiation. Clarendon Press., 1954, 430 p. (Russian edition: Gaitler V. *Kvantovaya teoriya izlucheniya* [The Quantum Theory of Radiation]. Moscow, Izdatel'stvo inostrannoi literatury, 1956, 492 p.).

Katsnelson B.V., Kalugin A.M., Larionov A.S. *Elektrovakuumnye elektronnye i gazorazryadnye pribory: spravochnik* [Electric Vacuum and Gas-Electronic Devices: Handbook]. Moscow, Radio i Svyaz' Publ., 1985, 864 p. (in Russian).

Lidvansky A.S., Chaerdinov N.S. The dynamics of cosmic rays in the electrostatic field of the atmosphere and the generation of particles thunderclouds // Bulletin of The Russian Academy of Sciences: Physics. 2007, vol. 71, no. 7, pp. 1060–1062 (in Russian).

Matveev L.T. *Kurs obshchei meteorologii* [The Course of General Meteorology]. Leningrad, Gidrometeoizdat Publ., 1984, 752 p. (in Russian).

Maurchev E.A., Balabin Y.V., Gvozdevsky B.B., Vashenyuk E.V. A new numerical model for investigating cosmic rays in the Earth's atmosphere // Bulletin of The Russian Academy of Sciences: Physics. 2015, vol. 79, no. 5, pp. 657–659. DOI: 10.3103/S1062873815050305.

Mendonça R.R.S. de, Raulin J.-P., Bertoni F.C.P., et al. Long-term and transient time variation of cosmic ray fluxes detected in Argentina by CARPET cosmic ray detector // J. Atmos. Solar-Terr. Phys. 2011, vol. 73. pp. 1410–1416. DOI: 10.1016/j.jastp. 2010.09.034.

Rust W.D., Trapp R.J., Initial balloon soundings of the electric field in winter nimbostratus clouds in the USA // Geophys. Res. Lett. 2012, vol. 29, pp. 1959–1962. DOI: 10.1029/ 2002GL015278.

Shishaev V.A., Beloglazov M.I. An automatic recorder of atmospheric precipitations // Instruments and Experimental Techniques. 2011, vol. 54, no. 2, pp. 291–293. DOI: 10.1134/ S0020441211020084.

Vashenyuk E.V., Balabin Yu.V., Germanenko A.V., Gvozdevsky B.B. Study of radiation related with atmospheric precipitations // Proceedings of ICRC-2011. 2011, vol. 11, id 0328, pp. 360–363.

The article is based on materials of the XIVth Young Scientists' Conference "Interaction of fields and radiation with matter" of Baikal Young Scientists' International School on Fundamental Physics (September 14–18, 2015, Irkutsk, Russia)